An improved calculation method for fiber Raman amplifier equations with multi-wavelength pumping

Jianhua Chang (常建华), Mingde Zhang (张明德), and Xiaohan Sun (孙小菡)

Department of Electronic Engineering, Southeast University, Nanjing 210096

Received January 15, 2004

A novel numerical method for fiber Raman amplifier (FRA) from standard propagation equations is presented and derived based on the one-step method for ordinary differential equation (ODE). The proposed algorithm is effective in solving FRA equations including all the interactions among pumps, signals, and noises. Applications of the numerical analysis to practical FRA-based systems show a great reduction in computation time in comparison with the average power method and the fourth-order Runge-Kutta (RK) method, under the same condition. Also the proposed method can decrease the computing time over three orders of magnitude with excellent accuracy promises in comparison with the direct integration method.

OCIS codes: 060.2320, 060.4230, 140.4480.

With the advance of high-power laser diode technology, fiber Raman amplifier (FRA) has become a practical choice to meet the increasing demands of transmission capacity and distance of optical fiber communication systems. In addition to its distinctive flexibility in gain-band allocation, the gain bandwidth of FRA also can be easily extended with the inclusion of multiple pumps. Seemingly simple in principle, the optimization process for the gain-bandwidth design for FRA in a real wavelength division multiplexing (WDM) system requires extensive efforts with more considerations on many factors, such as pump interaction, polarization dependency, double Rayleigh scattering, and detailed information on fiber parameters. In the design of ultra-broad bandwidth FRA with multiple pumps, however, it needs exhaustive computing time to achieve well-behaved results by using direct integration of coupled equations. The required simulation time may make the design be unpractical if the bandwidth is large enough and transmission fiber length is long enough. Fortunately, many practical methods are proposed[1−4]. Reference [1] provided a direct Runge-Kutta (RK) method which had taken into account of all factors such as signals, pumps, noises, and Rayleigh scattering, etc.. Reference [2] obtained an efficient method with an average power analysis, which reduced the computing time of over two orders of magnitude compared with the direct integration approach based on ordinary coupled differential equations. Liu *et al.*[3,4] proposed a multi-step method which could availably increase the precision and stability in designing FRA compared with the average power method. Although some of these methods can compute the generalized differential equation system of FRA with excellent accuracy promises, they are mostly high-memory demand and much complex.

In this paper, we provide a novel analysis for ultrabroad-band FRA design with multiple pumps. The proposed algorithm is effective in solving FRA equations that include pumps, signals, noises, and their backscattering waves. Simulation results show that, in designing the FRA, our method can effectively improve the accuracy and stability with decreased computing time in comparison with the methods in Refs. [1,2].

The analysis of distributed Raman amplifier (DRA) is based on a set of coupled steady-state equations that include spontaneous Raman emission and its temperature dependence, Rayleigh scattering including multiple reflections, amplified spontaneous emission (ASE), stimulated Raman scattering (SRS), high order Stokes generation, and arbitrary interactions between an unlimited number of pumps and signals. The forward and backward evolution of pumps, signals and ASE powers can be expressed in terms of the following equations[2−6]

$$\begin{aligned}\frac{\mathrm{d}P^{\pm}(z,\nu_i)}{\mathrm{d}z} &= \mp\alpha(\nu_i)P^{\pm}(z,\nu_i) \pm \eta(\nu_i)P^{\pm}(z,\nu_i)\\ &\pm P^{\pm}(z,\nu_i)\sum_{m=1}^{i-1}\frac{g_R(\nu_m-\nu_i)}{\Gamma A_{\mathrm{eff}}}[P^{\pm}(z,\nu_m)+P^{\mp}(z,\nu_m)]\\ &\pm h\nu_i\sum_{m=1}^{i-1}\frac{g_R(\nu_m-\nu_i)}{\Gamma A_{\mathrm{eff}}}[P^{\pm}(z,\nu_m)+P^{\mp}(z,\nu_m)]\\ &\times[1+(\mathrm{e}^{\frac{h(\nu_m-\nu_i)}{kT}}-1)^{-1}]\Delta\nu\\ &\mp P^{\pm}(z,\nu_i)\sum_{m=i+1}^{n}\frac{\nu_i}{\nu_m}\frac{g_R(\nu_i-\nu_m)}{\Gamma A_{\mathrm{eff}}}\\ &\times[P^{\pm}(z,\nu_m)+P^{\mp}(z,\nu_m)]\\ &\mp 2h\nu_i P^{\pm}(z,\nu_i)\sum_{m=i+1}^{n}\frac{\nu_i}{\nu_m}\frac{g_R(\nu_i-\nu_m)}{\Gamma A_{\mathrm{eff}}}\\ &\times[1+(\mathrm{e}^{\frac{h(\nu_i-\nu_m)}{kT}}-1)^{-1}]\Delta\mu, \end{aligned} \tag{1}$$

where $P^{+}(z,\nu_i)$ and $P^{-}(z,\nu_i)$ are optical powers of forward- and backward-propagating waves within infinitesimal bandwidth around frequency ν_i, respectively. α, η, h, k, and T are attenuation coefficient, Rayleigh-backscattering coefficient, Planck's constant, Boltzmann constant, and temperature, respectively. A_{eff} is the effective area of optical fiber at frequency ν_m, $g_{\mathrm{R}}(\nu_m-\nu_i)$ is Raman gain parameter at frequency ν_i

due to pump at frequency ν_m[7,8]. The factor Γ accounts for polarization randomization effects, whose value lies between 1 and 2. In $\sum$ terms, $m = 1$ to $m = i - 1$ and $m = i + 1$ to $m = n$ explain amplifications or attenuations for the channels at frequency ν_i, respectively. $\Delta\mu$ and $\Delta\nu$ are the noise spectral intervals for the noise increases or decreases in the calculation (in this letter, they are assumed to be equal). The first two terms in the right hand of Eq. (1) denote the fiber loss and Rayleigh back-scattering, the third term denotes the Raman gain due to shorter wavelength, the fourth term denotes the ASE noise with thermal factor, the fifth term denotes the pump depletion due to longer wavelength, and the sixth term denotes the loss due to noise emission[8].

For the mathematical convenience, Eq. (1) is rewritten as[3,4]

$$\frac{\mathrm{d}P^{\pm}(z,\nu_i)}{\mathrm{d}z} = P^{\pm}(z,\nu_i)F(z,\nu_i), \tag{2}$$

where

$$F(z,\nu_i) = \mp\alpha(\nu_i) \pm \eta(\nu_i) \mp \sum_{m=i+1}^{n} \frac{\nu_i}{\nu_m} \frac{g_{\mathrm{R}}(\nu_i - \nu_m)}{\Gamma A_{\mathrm{eff}}}$$

$$\times [P^{\pm}(z,\nu_i) + P^{\mp}(z,\nu_i)$$

$$+2h\nu_i \left(1 + (\mathrm{e}^{\frac{h(\nu_i-\nu_m)}{kT}} - 1)^{-1}\right)\Delta\mu]$$

$$\pm \sum_{m=1}^{i-1} \frac{g_{\mathrm{R}}(\nu_m - \nu_i)}{\Gamma A_{\mathrm{eff}}} [P^{\pm}(z,\nu_i) + P^{\mp}(z,\nu_i)]$$

$$\times \left[1 + \frac{h\nu_i}{P^{\pm}(z,\nu_i)} \left(1 + (\mathrm{e}^{\frac{h(\nu_m-\nu_i)}{kT}} - 1)^{-1}\right)\Delta\nu\right]. \tag{3}$$

To solve Eq. (2), we divide the fiber length into many segments with section length of Δz. In Ref. [2], the average power analysis technique was applied. This technique was one-step method, which involves information from one of the previous mesh point, z_j. This method could greatly decrease the computing time. According to the method, Eq. (2) can be solved as

$$P^{\pm}(z_{j+1},\nu) = P^{\pm}(z_j,\nu)\exp[F(z_j,\nu)\Delta z], \tag{4}$$

where Δz is the step size for each elemental amplifier section.

Here we present a novel method to more effectively solve Eq. (1). Assuming that

$$P^{\pm}(z_{j+1},\nu) = P^{\pm}(z_j,\nu)\exp[(k_1 + k_2)\Delta z/2],$$

$$k_1 = F(z_j,\nu), \quad \text{and} \quad k_2 = F(z_j + \Delta z,\nu),$$

we can find that our method uses functional evaluation information at points between z_j and z_{j+1} to obtain an approximate solution of the mesh point, z_{j+1}. Roughly, it looks as if our method may cost the computing time as about two times as the average power method, but its accuracy and stability is evident and then the step size can be enlarged. In fact, the method can effectively decrease the computing time under the same accuracy compared with the average power method and the fourth-order RK method. This method can be applied to real system performance evaluations.

In order to compare the accuracy of our method with that of average power method in Ref. [2] and fourth-order RK method in Ref. [1], an ordinary differential equation is tested, i.e.,

$$\frac{\mathrm{d}y}{\mathrm{d}t} = y\left(\frac{t^3}{200} + \frac{t^2}{50} + t\right),$$

$$y(0) = 1, \quad \text{and} \quad t \in [0, 3.6]. \tag{5}$$

The exact solution for Eq. (5) is

$$y = \exp(t^4/800 + t^3/150 + t^2/2). \tag{6}$$

Substituting $y(t)$ and $(\frac{t^3}{200} + \frac{t^2}{50} + t)$ of Eq. (5) into $P^{\pm}(z,\nu)$ and $F(z,\nu)$ of Eqs. (2) and (4), we can obtain Fig. 1. Lines with square, triangular, asterisk, and circle symbols are the results obtained from the exact solution, our novel method, the average power method, and the fourth-order RK method, respectively. From Fig.1 we can see that, under the same step size h, our proposed method has the most high accuracy. Simulation results also show that, even the step size h of average power method is half of our method, it still cannot reach the same accuracy.

Figure 2 illustrates relative errors between the numerical values and exact solution. Under the same step size of $h = 0.1$, the relative error between our method and exact solution is the smallest and keeps almost the same values remaining as small as 10^{-4} with increase of t, while that of the average power method grows almost linearly and

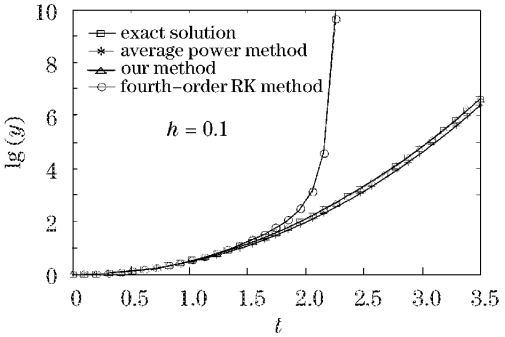

Fig. 1. Accuracy comparison of our method, fourth-order RK method, and average power method with exact solution.

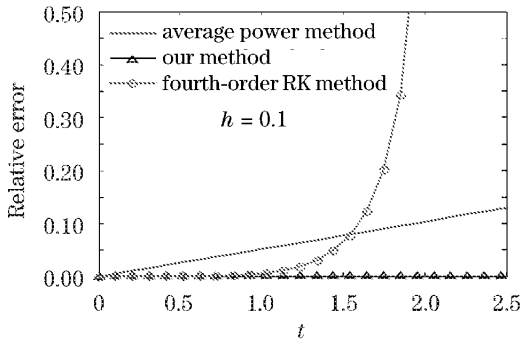

Fig. 2. Relationship of relative error with t.

when $t >\sim 2$ the error of the fourth-order RK method expands considerably and is then divergent.

Although our method costs computing time as about two times as the average power method, its accuracy (see Figs. 1 and 2) is evident, and then the step size can be enlarged, if its accuracy margin is big enough. Hence, the computing time in our method can be reduced with a little sacrifice of accuracy. As to the fourth-order RK method, we can obviously see that the computing time of our method is just half of that, while the accuracy is more higher. Therefore, we can conclude that, in fact, our novel method has considered the computing speed and the accuracy comprehensively and it can be effectively applied to real system performance evaluations.

To calculate noise figure, we start from the fundamental propagation Eq. (1) and rearrange power dependent terms (Eqs. (8)−(11): A, B, C, and D), and reduce the propagation equations to a much simpler form as in Ref. [2]

$$\frac{\mathrm{d}P^{\pm}(z,\nu_i)}{\mathrm{d}z} = \pm\{[-\alpha(\nu_i) + A(z,\nu_i) - C(z,\nu_i) - D(z,\nu_i)]P^{\pm}(z,\nu_i) + B(z,\nu_i) + \eta(\nu_i)P^{\pm}(z,\nu_i)\}, \quad (7)$$

$$A(z,\nu_i) = \sum_{m=i+1}^{n} \frac{g_{\mathrm{r}}(\nu_m - \nu_i)}{\Gamma A_{\mathrm{eff}}}[P^{\pm}(z,\nu_m) + P^{\mp}(z,\nu_m)], \quad (8)$$

$$B(z,\nu_i) = h\nu_i \sum_{m=i+1}^{n} \frac{g_{\mathrm{r}}(\nu_m - \nu_i)}{\Gamma A_{\mathrm{eff}}} \times [P^{\pm}(z,\nu_m) + P^{\mp}(z,\nu_m)]\left[1 + (\mathrm{e}^{\frac{h(\nu_m-\nu_i)}{kT}} - 1)^{-1}\right]\Delta\nu, \quad (9)$$

$$C(z,\nu_i) = \sum_{m=1}^{i-1} \frac{\nu_i}{\nu_m} \frac{g_{\mathrm{r}}(\nu_i - \nu_m)}{\Gamma A_{\mathrm{eff}}}[P^{\pm}(z,\nu_m) + P^{\mp}(z,\nu_m)], \quad (10)$$

$$D(z,\nu_i) = 2h\nu_i \sum_{m=1}^{i-1} \frac{\nu_i}{\nu_m} \frac{g_{\mathrm{r}}(\nu_m - \nu_i)}{\Gamma A_{\mathrm{eff}}} \times [P^{\pm}(z,\nu_m) + P^{\mp}(z,\nu_m)]\left[1 + (\mathrm{e}^{\frac{h(\nu_i-\nu_m)}{kT}} - 1)\right]\Delta\mu, \quad (11)$$

$$G_i(L) = \exp\{\int_0^L [-\alpha(\nu_i) + A(z,\nu_i) - C(z,\nu_i) - D(z,\nu_i)]\mathrm{d}z\}, \quad (12)$$

where $P^{+}(z,\nu_i)$, $P^{-}(z,\nu_i)$, α, η, h, k, Γ, and T are the same meanings as in Eq. (1). $G_i(L)$ is the gross gain of the ith signal. Thus the noise figure can be given by

$$F_i = \frac{1}{G_i(L)} + \frac{2}{h\nu_i\Delta\nu}\int_0^L \frac{B_i(z) + \eta(\nu_i)P^{\pm}(z,\nu_i)}{G_i(z)}\mathrm{d}z. \quad (13)$$

For WDM systems, the "shooting method" is usually used to solve such two-point boundary problem. In this paper, we take the following iterative steps. First, we calculate the backward propagation pump power distribution along the fiber, without taking account of the attenuation caused by signals. In this process, the pump attenuation is only caused by the linear attenuation of fiber. Next, we calculate the forward propagation signal power distribution. This time we have already got pump power distribution along the fiber, so signals suffer not only fiber attenuation but also the gain caused by pumps. Then we calculate the backward propagation pump power distribution along the fiber with taking account of the attenuation caused by signals. Thus we get another pump power distribution along the fiber and average the former two pump powers with a weighting factor. When we go on to calculate the signal propagation power, we use the averaged pump power. Repeat these iterative steps until a promised precision is approached. Commonly the weighting factor can be taken to be 1/6 and after 6 or 7 times iterations, a precision of 10^{-4} can be approached.

In simulation, the used parameters are given as follows. $L = 10$ km, $T = 300$ K, $\alpha_p = 0.3$ dB/km, $\alpha_s = 0.2$ dB/km, $G = 20$ dB, $\eta = -38$ dB/km, $N = 100$ (from 1510 to 1610 nm with the channel spacing of 1 nm), $A_{\mathrm{eff}} = 50\ \mu\mathrm{m}^2$, $\Gamma = 2$. The pump wavelength are 1404, 1413, 1431, 1449, 1463, and 1495 nm, and the corresponding optimal pump powers are 680, 600, 440, 190, 76, and 45 mW, respectively[9].

Figure 3 shows the on-off gain of the output signals transmitting along the fiber of 10 km and noise figure, which are calculated from our method and the average power method, respectively. The solid line is from our method with 10 fiber sections while the dashed line comes from the average power method with 80 fiber sections, respectively. It can be seen that, although with almost the same precision, the iterative steps of our method are much longer than the average power method. So the computing time can be reduced to about one seventh compared our method with average power method. According to Ref. [2], the average power method can

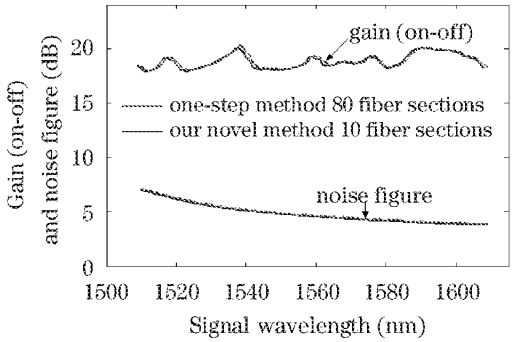

Fig. 3. The calculated signal optical gains and noise figures.

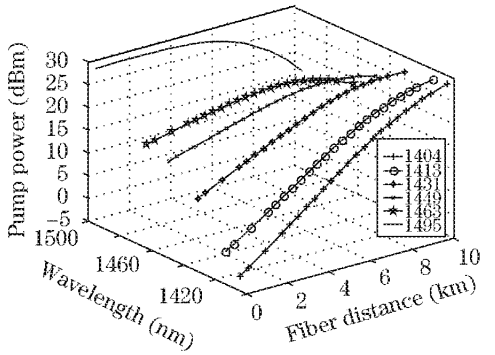

Fig. 4. Pump power evolution along the fiber in the DRA.

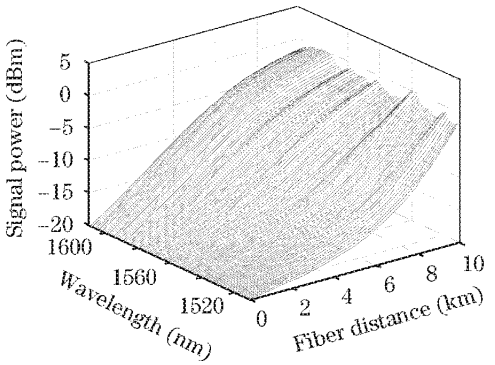

Fig. 5. Signal power evolution along the fiber in the DRA.

reduce the computing time of over two orders of magnitude compared with the direct integration approach based on ordinary coupled differential equations[3]. Therefore, our proposed method can decrease the computing time of over three orders of magnitude in comparison with the standard integration approach.

Figures 4 and 5 exhibit powers of pumps and signals along the fiber. From Fig. 4, we can see that the interaction of different pump waves is significant, which will cause amplification of some pumps before they are depleted by signals. Both Figs. 4 and 5 show that there is strong interaction between the pumps and signals due to SRS.

In fact, our novel method is the second-order of Our-Runge-Kutta (ORK) method in Ref. [10]. The numerical calculations show that our proposed method is superior to average power method and the fourth-order RK method in the accuracy. Theoretically, the accuracy can increase with the order of ORK. On the other hand, the more the order of ORK is, the more the computing time costs under the same number of steps. In general, our method can availably improve the accuracy and decrease the computing time with larger step sizes. Actually, we find that the second-order ORK is better than other order ORK at giving consideration to the accuracy and computing time.

In conclusion, we propose a fast and accurate numerical method for ultra-broad bandwidth FRA design with multiple pumps. Also we have successfully derived the noise figure function from the standard propagation equations. Employing this method, output signal gain spectra, pump power and signal power distributions along the fiber have been simulated. Simulation results show that, compared with the direct integration method of ordinary coupled differential equations, our proposed method can decrease the computing time with excellent accuracy. Additionally, the method can improve the accuracy in comparison with the average power method, also it can remarkably decrease the computing time compared with the fourth-order RK method. The method can be further used to optimize the design of FRA.

J. Chang's e-mail address is jianhuachang@seu.edu.cn.

References

1. J. H. Chang, M. D. Zhang, and X. H. Sun, Chin. J. Lasers (in Chinese) **31,** 579 (2004).
2. B. Min, W. J. Lee, and N. Park, IEEE Photon. Technol. Lett. **12,** 1486 (2000).
3. X. M. Liu, H. Y. Zhang, and Y. L. Guo, IEEE Photon. Technol. Lett. **15,** 392 (2003); X. M. Liu, IEEE Photon. Technol. Lett. **15,** 1321 (2003).
4. X. M. Liu and B. Lee, Opt. Express **11,** 2163 (2003).
5. Y. Emory and S. Namiki, in *Tech. Dig. OFC'99* **2,** (1999).
6. S. Wang, C. Fan, and C. C. Fan, in *2002 International Conference on Communication Technology Proceedings, WCC-ICCT* **2,** 1550 (2000).
7. S. Namiki and Y. Emori, IEEE J. Sel. Top. Quantum Electron. **7,** 3 (2001).
8. G. P. Agrawal, *Nonlinear Fiber Optics* (2nd edition) (San Diego, Academic Press, 1995).
9. X. Zhou, C. Lu, P. Shum, and T. H. Cheng, IEEE Photon. Technol. Lett. **13,** 945 (2001).
10. X. M. Liu and B. Lee, Opt. Express **11,** 1452 (2003).